Maternal Inactivity Programs Skeletal Muscle Dysfunction in Offspring Mice by Attenuating Apelin Signaling and Mitochondrial Biogenesis

Jun Seok Son[1,3], **Song Ah Chae**[1], **Hongyang Wang**[2], **Yanting Chen**[1], **Alejandro Bravo Iniguez**[4], **Jeanene M. de Avila**[1], **Zhihua Jiang**[1], **Mei-Jun Zhu**[4], **Min Du**[1,3,5,*]

[1]Nutrigenomics and Growth Biology Laboratory, Department of Animal Sciences, Washington State University, Pullman, WA 99164, USA

[2]Institute of Animal Husbandry and Veterinary Science, Shanghai Academy of Agricultural Sciences, Shanghai, China

[3]School of Molecular Biosciences, Washington State University, Pullman, WA 99164, USA

[4]School of Food Science, Washington State University, Pullman, WA 99164, USA

[5]Lead Contact

SUMMARY

Although maternal exercise (ME) becomes increasingly uncommon, the effects of ME on offspring muscle metabolic health remain largely undefined. Maternal mice are subject to daily exercise during pregnancy, which enhances mitochondrial biogenesis during fetal muscle development; this is correlated with higher mitochondrial content and oxidative muscle fibers in offspring muscle and improved endurance capacity. Apelin, an exerkine, is elevated due to ME, and maternal apelin administration mirrors the effect of ME on mitochondrial biogenesis in fetal muscle. Importantly, both ME and apelin induce DNA demethylation of the peroxisome proliferator-activated receptor γ coactivator-1α (*Ppargc1a*) promoter and enhance its expression and mitochondrial biogenesis in fetal muscle. Such changes in DNA methylation were maintained in offspring, with ME offspring muscle expressing higher levels of PGC-1α1/4 isoforms, explaining improved muscle function. In summary, ME enhances DNA demethylation of the *Ppargc1a* promoter in fetal muscle, which has positive programming effects on the exercise endurance capacity and protects offspring muscle against metabolic dysfunction.

In Brief

Son et al. demonstrate that maternal exercise facilitates fetal muscle development, which improves muscle function and exercise endurance in offspring. Maternal administration of apelin, an exerkine, mirrors the beneficial effects of maternal exercise on mitochondrial biogenesis and fetal muscle development. These findings suggest apelin and its receptor as potential drug targets for improving fetal muscle development of sedentary mothers.

Graphical Abstract
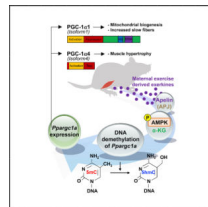
INTRODUCTION

Obesity is a worsening problem worldwide, which is accompanied with complications such as type 2 diabetes mellitus, cardiovascular diseases, and sarcopenia (Kim et al., 2010; Neeland et al., 2012). More importantly, both epidemiological and animal studies show an inherent link between maternal obesity and metabolic diseases in their progeny (McCurdy et al., 2009). Skeletal muscle accounts for about 40% of body weight, which is not only essential for physical movement but also key to the use of glucose and lipids (Richter and Hargreaves, 2013). Moreover, obesity leads to dysfunction of mitochondria in the skeletal muscle, accelerating age-associated muscle disorders, including sarcopenia (Kalinkovich and Livshits, 2017; Roy et al., 2016). Physical activity protects muscle mitochondrial malfunction and atrophy due to diet-induced obesity (Menshikova et al., 2007; Roy et al., 2016), increases basal metabolic rates (BMRs), and prevents metabolic syndromes (Heo et al., 2017). Recently, maternal exercise (ME) was shown to improve the metabolic health of offspring born to obese maternal mice (Stanford et al., 2017). However, the mechanistic links between ME and fetal muscle development and their long-term impacts on offspring muscle function and metabolic health remain to be explored.

Peroxisome proliferator-activated receptor g coactivator-1α (gene, *Ppargc1a*; protein, PGC-1α) is a master regulator of mitochondrial biogenesis. As a transcriptional coactivator, PGC-1α is strongly activated due to exercise (Ruas et al., 2012). In skeletal muscle, two major PGC-1α isoforms have been identified: a full-length isoform (isoform 1) mainly mediating mitochondrial biogenesis and a 37-kD truncated isoform mainly mediating angiogenesis and muscle hypertrophy (isoform 4) (Ruas et al., 2012). The expression of the *Ppargc1a* gene is regulated by DNA methylation of its promoter, and the methylation status is elevated by consumption of a high-fat diet (HFD) but suppressed due to exercise (Laker et al., 2014). Because ME is becoming increasingly uncommon and maternal inactivity prevails (Archer et al., 2013), we hypothesized that maternal lack of exercise alone permanently suppresses the expression of *Ppargc1a*, which programs muscle dysfunction in offspring. In

addition, ME stimulates the secretion of an exerkine, apelin, which has been implicated for its regulatory roles in placental and fetal development (Ho et al., 2017; Son et al., 2019b). We additionally hypothesized that apelin administration during pregnancy can mimic the beneficial role of ME on fetal muscle development.

Thus, the objective of the current study was to examine the impacts of ME on fetal muscle development, offspring muscle fiber type composition, and metabolic capacity and to further explore apelin-mediated DNA hypomethylation in the *Ppargc1a* gene as a critical mechanism linking ME to muscle metabolic dysfunction in offspring. Because exercise is highly accessible, exploring mechanisms underlying the improvement of offspring muscle function due to ME has high clinical implications in curbing obesity and improving the metabolic health of the next generations.

RESULTS

ME Enhances Muscle Functional Capacity of Offspring

At weaning, offspring were subjected to a single bout of endurance exercise. Following an acute graded aerobic treadmill running test (Figure S1A), offspring from exercised mothers (M- Ex) showed elevated oxygen consumption rates (OCRs) and carbon dioxide production rates during exercise (Figures S1B–S1E). The maximal OCR (VO_2 max) and total exercise time and distance were further significantly increased in M-Ex offspring (Figure 1B). We additionally measured relative upper limb grip strength as an indicator of muscle functional capacity (Son et al., 2019a). The forelimb maximal grip strength and endurance capacity of weanling mice were not different between treatments (Figures 1C and 1D). Importantly, following 2 months of HFD treatment, the elevated OCRs and exercise endurance in M-Ex offspring were maintained (Figure 1E). The forelimb maximal strength and endurance under ten times of repeated grip measurements were higher in M-Ex offspring, showing improved muscle force and exercise endurance capacity (Figures 1F and 1G). When comparing M-Ex offspring fed with HFD and control diet (CD), we found that HFD offspring had lower grip strength (Figure 1F). These data show the long-term protective effects of ME on the endurance strength of offspring mice challenged with HFD.

ME Regulates Muscle Fiber Type Compositions and Cross-Sectional Areas of Offspring

Morphologically, both female and male M-Ex weanling offspring had higher capillary densities in the soleus muscle, dominant with oxidative fibers, and tibialis anterior (TA), dominant with glycolytic fibers (Figures S2A and S2B). These enhancements were sustained after 2 months of HFD challenge, but no difference between maternal control (M-Ctrl) and maternal exercise (M-Ex) fed a CD was found, showing that ME protected against capillary impairment due to HFD challenge (Figures 2A–2C). The proportion and size of oxidative fibers, especially type I muscle fibers, were analyzed in the central and lateral areas of TA muscles of offspring (Figures S2C–S2G; Figures 2D–2H). The ratios of type I and IIa fibers were increased in both central and lateral locations of TA muscle of weanling and HFD challenged mice (Figures S2C–S2G; Figures 2D–2H). Consistently, M-Ex elevated type IIa mRNA expression in weanling and HFD-fed offspring (Figures S2H and S2I; Figures 2I and 2J). Furthermore, IIa expression was decreased and IIb expression was increased in response

to HFD challenge compared to CD in male offspring (Figure 2J). In agreement, ME increased muscle weight of both weanling and HFD challenged offspring mice (Figures S3A, S3B, and S3F), which was associated with increased cross-sectional areas (CSAs) in TA muscles (Figures S2C–S2G; Figures 2D–2H). Taken together, these data demonstrate that ME increases the number of oxidative muscle fibers in the skeletal muscle of female and male offspring mice at weaning and also after challenged by HFD, demonstrating the programming effects of ME on oxidative function and exercise endurance of offspring muscle.

ME Induces Mitochondrial Biogenesis and Oxidative Phosphorylation in Fetal and Offspring Mice

Mitochondrial function correlates with endurance capacities of the skeletal muscle (Granata et al., 2016). The mitochondrial DNA (mtDNA) copy number was higher in fetal muscle and the gastrocnemius muscle of the weanling (Figure 3A; Figure S3C), and maintained after HFD challenge (Figure 3D). Moreover, the mRNA expression of mitochondrial marker, *Tfam* was also elevated in M-Ex of both female and male weanling and HFD challenged mice (Figure S3D; Figure 3F). Besides, ME elevated the protein levels of voltage-dependent anion channel (VDAC) and cytochrome C in M-Ex offspring after HFD challenge (Figure S3G). Morphologically, M-Ctrl offspring challenged with HFD showed impaired mitochondrial cristae compared to M- Ex offspring (Figure 3G). Moreover, the sizes of mitochondria were decreased in M-Ex compared to M-Ctrl offspring (Figure 3G). Consistently, mitochondrial fission regulator, Drp1 phosphorylation t was lower in M-Ctrl challenged with HFD, but protected in M-Ex offspring (Figure 3H).

To explain whether the difference in mitochondrial density had a fetal origin, mitochondrial related markers were further analyzed in fetal muscle. Compared to M-Ctrl fetuses, the expression of mitochondrial-biogenesis-related genes including *Ppargc1a*, *Cox7a1*, *Tfam*, *Tfb1m*, *Tfb2m*, and *Nrf1* was higher in both female and male M-Ex fetal muscle (Figure 3C). Notably, mRNA expression of *Ppargc1a* was elevated in the M-Ex gastrocnemius muscle at weaning and after HFD challenge (Figure S3E; Figure 3E). Furthermore, expression of the PGC-1α1 isoform enhances muscle oxidative capacity, whereas the PGC-1α4 isoform enhances muscle hypertrophy (Ruas et al., 2012). Consistently, protein levels of PGC-1α1 and 4 were elevated in both M-Ex female and male fetal muscle (Figure 3B). However, the PGC-1α1 and α4 isoforms did not differ between treatments challenged with CD (Figure 3I). Following HFD challenge, on the other hand, α1 and α4 isoforms were protected from downregulation in M-Ex compared to M-Ctrl offspring (Figure 3I). Taken together, these data show that ME stimulates fetal PGC-1α expression, which has persistent effects on PGC-1α expression in offspring both before and after HFD challenge.

Exogenous Apelin Administration Mimics the Beneficial Effects of ME on Mitochondrial Biogenesis in Fetal Skeletal Muscle

Exercise stimulates skeletal muscle apelin expression, and apelin, binding to its G protein-coupled receptor APJ activates AMP-activated protein kinase (AMPK) to enhance metabolic homeostasis and mitochondrial biogenesis (Than et al., 2015; Vinel et al., 2018). Consistently, we found that ME highly elevated apelin expression in fetal and weanling

muscle (Figure S4A), and these enhancements sustained following 2 months of CD/HFD challenge, consistent with APJ activation in adult muscle (Figures S4B and S4C). AMPK was activated in ME fetal muscle (Figure S4D). To test whether apelin mediates AMPK activation and stimulates *Ppargc1a* expression in ME fetal muscle, pregnant mice were subjected to daily apelin supplementation (APN) or PBS injection (intraperitoneal [i.p.]) (embryonic day 1.5 [E1.5] to E16.5) (Figure 4A). Consistent with the ME study, mtDNA copy number of female and male fetal muscle was increased in the APN group compared to the PBS group (Figure 4B). Furthermore, APN enhanced mitochondrial-biogenesis-related gene expression (Figure 4C) and AMPK phosphorylation (Figure S4E) in female and male fetal muscles. In agreement with ME fetal muscle, PGC-1α isoforms α1 and 4 were robustly activated in APN compared to those of the PBS injection treatment (Figure 4D).

To explore the mediatory roles of apelin receptor (APJ) signaling, we used myogenic cells from a whole-body knockdown animal model, β-actin^{Cre}/$Apj^{flox/+}$ (KD^{Apj}) mice, which were treated with apelin (Figure 4E). Here, we used hemizygous APJ knockout due to the lethality associated with homozygous APJ knockout. In agreement, APJ protein levels were downregulated in KD^{Apj} cells of both females and males (Figure 4F). As a result of APJ downregulation, mitochondrial biogenic markers *Ppargc1a*, *Tfam*, *Tfb1m*, *Tfb2m*, and *Cox7a1* were highly suppressed in female and male myogenic cells (Figure 4G). Furthermore, the protein levels of PGC-1α1 and 4 isoforms were decreased in response to APJ knockdown in female and male myogenic cells (Figure 4H). Taken together, these data demonstrate that apelin stimulates mitochondrial biogenesis in myogenic cells by activation of APJ. Furthermore, AMPK activation was suppressed in APJ-deficient myogenic cells (Figure S4F).

To further analyze the mitochondrial function that resulted from apelin administration, we performed next-generational RNA sequencing analysis using whole-transcriptome termini site (WTTS) sequencing, showing that APN supplementation during pregnancy enhanced fetal muscle development, protein synthesis, and mitochondrial respiratory capacity (Figure 5). Taken together, these data demonstrate that ME stimulates apelin signaling and AMPK activity by APJ activation, which enhances *Ppargc1a* expression and mitochondrial biogenesis and improves metabolic function.

ME Stimulates *Ppargc1a* Expression by AMPK/α-KG-Mediated DNA Demethylation in Its Promotor

In our previous study, we reported that AMPK-dependent α-ketoglutarate (α-KG) production promotes the conversion of 5-methylcytosine (5mC) to 5-hydroxymethylcytosine (5hmC) in gene promoters, which is catalyzed by ten-eleven translocation hydroxylases (TETs) (Yang et al., 2016). In agreement, the ratio of α-KG to 2-hydroxyglutarate (2-HG), a competitive inhibitor of TETs, was elevated in the fetal skeletal muscle (Figure 6A). To explore potential DNA methylation changes enhancing *Ppargc1a* expression, three specific regions in the *Ppargc1a* promoter were selected based on CpG enrichment (Figure 6B). Consistent with increased *Ppargc1a* expression (Figures 3C and 3E; Figure S3E), the DNA methylation (5mC) in these three regions was decreased in the skeletal muscle of both female and male fetuses of M-Ex, whereas the DNA demethylation intermediate (5hmC)

was increased (Figure 6C). Importantly, such changes persisted in the muscle of both female and male M-Ex offspring following HFD challenge (Figure 6E). On the other hand, post-weaning HFD challenge slightly increased the methylation level (5mC) compared to that of offspring mice fed the CD (Figure 6D).

Similarly, changes in DNA methylation of the *Ppargc1a* promoter were negatively associated with apelin expression in fetal muscle due to ME (Figures S5C and S5D). APN during pregnancy reduced 5mC but increased 5hmC levels in female and male fetal muscles (Figure 6F), showing a negative correlation between 5mC and *Ppargc1a* gene expression (Figures S5E and S5F), which was consistent with data of M-Ex muscle. AMPK activity further correlated with serum apelin concentration in response to APN administration (Figures S5A and S5B). Taken together, these data show that ME increases AMPK activity and α-KG contents, likely through elevating apelin secretion, which enhances DNA demethylation in the promoter of the *Ppargc1a* gene and persistently elevates *Ppargc1a* expression in offspring muscle (Figure 6G).

DISCUSSION

Maternal adaptation to adverse environmental stimuli has been associated with various physiological changes in the offspring (Power and Schulkin, 2013), including a predisposition of offspring to the development of obesity and type 2 diabetes mellitus (Godfrey et al., 2017). Physical exercise is highly accessible and a prominent therapeutic tool to combat diet-induced obesity in adults (Peres Valgas da Silva et al., 2019). Based on epidemiological studies, exercise during pregnancy is beneficial for maternal health and neonatal outcomes (Barakat et al., 2015; Davenport et al., 2018; Gustafsson et al., 2016; Nascimento et al., 2012), which is supported by animal and human studies (Clapp, 2006; Hopkins and Cutfield, 2011; Mangwiro et al., 2018; Moyer et al., 2016; Son et al., 2019b). However, these available studies focus on measurements of offspring outcomes due to ME of obese dams (Stanford et al., 2015, 2017). As a result, the impacts of ME on fetal development, especially skeletal muscle development, remain largely unexamined. Skeletal muscle accounts for 30%–40% of body weight (Janssen et al., 2000) and, as a whole, is the most important tissue for energy use. Muscle fibers are separated into glycolytic and oxidative fibers, with oxidative fibers especially rich in mitochondria and having high efficiency in their use of glucose and fatty acids (Chen et al., 2009; Lantier et al., 2014; Misu et al., 2017; Oberbach et al., 2006). Impaired development of fetal muscle due to maternal obesity or malnutrition programs metabolic dysfunction of muscle in progeny, predisposing offspring to obesity and metabolic diseases (Friedman, 2018; Tong et al., 2011b; Yan et al., 2010). In addition, poor skeletal muscle performance is correlated with exercise fatigue (Frisbee et al., 2019), which not only reduces the quality of life but also physical movement, worsening obesity and metabolic syndromes in offspring. In this study, we found that ME enhanced the oxidative capacity of offspring muscle by shifting muscle fiber types from glycolytic to oxidative without changing muscle weight, which might be associated with enhanced mitochondrial biogenesis (Chen et al., 2020). Consistently, we found that ME improved the endurance capacity of offspring muscle. Oxidative muscle fibers contain a high density of mitochondria, which was confirmed in offspring born to M-Ex.

In skeletal muscle, there are two major PGC-1α isoforms, the full-length PGC-1α1 mainly mediating mitochondrial biogenesis (Theilen et al., 2017) and the truncated PGC-1α4 isoform mediating angiogenesis and muscle hypertrophy (Ruas et al., 2012). The co-transcription function of PGC-1α1, commonly referring to as PGC-1α, is enhanced by endurance exercise training, which stimulates mitochondrial biogenesis and switches muscle fiber type composition (Lin et al., 2002; Wende et al., 2007) that is accompanied with switching from carbohydrates to lipids as the major source of energy during endurance exercise (Cantó et al., 2010). To explain phenotypic changes in offspring muscle due to ME, we analyzed the expression of PGC-1α. In alignment, the expression of PGC-1α was elevated in offspring muscle both at weaning and also after 2 months of HFD challenge, which is consistent with the enhanced mitochondrial density and oxidative capacity of offspring muscle due to ME. In addition, the expression of PGC-1α4 was also elevated in ME offspring. The higher concentration of PGC-1α4 provides an explanation for muscle hypertrophy in M-Ex offspring because PGC-1α4 inhibits the expression of muscle-specific ubiquitinases, activates insulin-like growth factor 1 (IGF-1), and inhibits myostatin expression (McPherron et al., 1997; Ruas et al., 2012; White et al., 2014).

AMPK is a master regulator of energy metabolism (Habegger et al., 2012; Hardie, 2007a, 2007b), which can be phosphorylated due to regular exercise, triggering the expression and phosphorylation of PGC-1α, which is a metabolic master regulator of mitochondrial biogenesis (Cantó et al., 2010; Menzies et al., 2013; Palacios et al., 2009; Sandri et al., 2006). Furthermore, increased PGC-1α activity suppresses the action of fork-head box class O 3 (FoxO3) that contributes to protein degradation and skeletal muscle atrophy (Sandri et al., 2006). Obesity induced by HFD inhibits AMPK activity and suppresses PGC-1α, impeding muscle development and regeneration (Fu et al., 2016). Accumulating evidence implicates the central regulatory role of AMPK in stem cell renewal and differentiation (Dzeja et al., 2011; Kang et al., 2013; Ochocki and Simon, 2013; Shah et al., 2010), which is likely associated with the ability of AMPK to promote PGC-1α-dependent oxidative transition (de Meester et al., 2014; Vazquez-Martin et al., 2013). Indeed, the transition to oxidative metabolism precedes changes in cell stemness and is required for differentiation (Folmes et al., 2011; Yu et al., 2013). Our previous studies show that low AMPK activity attenuates myogenic differentiation during muscle development (Tong et al., 2011b; Yan et al., 2010; Zhu et al., 2008) and that AMPK promotes myogenesis (Zhao et al., 2010, 2011). In addition, we observed pronounced upregulation of the AMPKα1 (gene name, *Prkaa1*) catalytic subunit (~33-fold) shortly after muscle injury, and AMPK was downregulated due to obesity, which impaired muscle regeneration (Fu et al., 2016). These studies emphasize the regulatory roles of AMPK in myogenesis and muscle development.

Furthermore, AMPK is an important mediator in epigenetic modifications, including DNA demethylation by increasing α-KG concentration (Yang et al., 2016). The α-KG is a rate-limiting cofactor required for TET-catalyzed DNA demethylation (Yang et al., 2016). Consistently, we found that AMPK and α-KG were inhibited due to maternal inactivity, which impeded DNA demethylation of the *Ppargc1a* promoter during fetal muscle development. Our data are in agreement with a previous report showing increased DNA methylation in the *Ppargc1a* promoter due to HFD (Laker et al., 2014). However, in that study, *Ppargc1a* DNA methylation was not examined during fetal development, leaving the

uncertainty of such change either due to the direct effects of ME on fetal development or derived from the presence of offspring obesity due to ME (Laker et al., 2014). In the present study, we demonstrate that ME, independent of post-weaning HFD, promotes DNA demethylation of the *Ppargc1a* promoter during fetal muscle development and protects offspring from impairment in skeletal muscle function due to HFD challenge.

Apelin is a peptide and an endogenous ligand for a G protein-coupled receptor, which is mainly expressed in the placenta, adipose tissue, and skeletal muscle in response to exercise (Otero-Díaz et al., 2018; Son et al., 2019b; Vinel et al., 2018). Furthermore, as downstream targets, apelin upregulates AMPK activity, which enhances mitochondrial biogenesis (Higuchi et al., 2007; Than et al., 2015) and the mitochondrial respiratory function (Attané et al., 2012), likely by stimulating PGC-1α expression (Hesselink et al., 2016). Consistently, chronic Pyrapelin 13 treatment of obese and insulin-resistant mice enhances glucose uptake and mitochondrial biogenesis in skeletal muscle (Dray et al., 2008). In our previous study, we found that ME enhanced apelin levels in fetal circulation and adipose tissues of both mothers and offspring (Son et al., 2020). Consistently, we observed the elevation of apelin in fetal and offspring muscle in this study, which correlated with AMPK activation and enhanced DNA demethylation in the *Ppargc1a* promotor. These data suggest that apelin elevation in fetal muscle due to ME might be a key mechanism improving mitochondrial biogenesis in fetal muscle, consistent with a previous study (Frier et al., 2009), and apelin signaling provides a molecular target for a therapeutic approach to improve fetal muscle development of physically inactive mothers.

Of note, there is concern about treadmill exercise as possible stress to maternal mice. Although acute exercise elicits stress temporally, both exercised and sedative maternal mice underwent the same protocol in this study, avoiding a possible interfe ence of stress. On the other hand, regular treadmill exercise at moderate intensity, which was used in the current study, actually has protective effects to stress-related symptoms (Loprinzi and Frith, 2019; Patki, 2014; Seo, 2018). There was no difference in gestation length and fetal weight at E18.5 (Son et al., 2019b, 2020). To avoid the possible de-training effects of ME to neonates, we stopped exercise on E18.5, allowing 2 days of interval before birth.

In summary, our data identify that ME activates AMPK and α-KG-mediated DNA demethylation in the promoter of the *Ppargc1a* gene, which persistently increases *Ppargc1a* expression in offspring muscle, correlated with enhanced oxidative capacity and exercise endurance. Thus, during fetal muscle development, DNA demethylation in the promoter of the *Ppargc1a* gene is a critical control point for improving offspring muscle functions. Although exercise is highly accessible, many mothers cannot do routine exercise for a variety of reasons. Exogenous apelin administration, therefore, may be an alternative and potential therapeutic strategy for improving the oxidative capacity and endurance of offspring muscle. Taken together, apelin administration to stimulate the *Ppargc1a* promoter DNA demethylation during fetal muscle development is a potential therapeutic strategy for uncoupling maternal inactivity with its programming effects on offspring skeletal muscle function, improving metabolic health of the next generations.

STAR★METHODS

Detailed methods are provided in the online version of this paper and include the following:

RESOURCE AVAILABILITY

Lead Contact—Further information and requests for resources and reagents should be directed to and will be fulfilled by the Lead Contact, Prof. Dr. Min Du (min.du@wsu.edu)

Materials Availability—This study did not generate any new unique reagents.

Data and Code Availability—Original data have been deposited to the NCBI Sequence Read Archive (SRA) repository: https://www.ncbi.nlm.nih.gov/bioproject/PRJNA674423/.

EXPERIMENTAL MODEL AND SUBJECT DETAILS

Animals—2-month-old C57BL/6J female mice were randomized and assigned into a control (CON) or an exercise (EX) group fed *ad libitum* with a conventional rodent diet (CD, Research Diets, New Brunswick, NJ, USA) (n = 6 per group). Females were mated with age-matched C57BL/6J males, and mating was confirmed by the presence of vaginal smear, which was designated as E0.5. At embryonic day 18.5 (E18.5), following 5 h fasting, pregnant females were anesthetized by carbon dioxide inhalation and euthanized by cervical dislocation as previously described (Son et al., 2019b). Fetal skeletal muscle tissues (collected from limbs after removing skin and primordial bone) were collected from one female and one male fetus of each pregnancy and stored at −80°C for further analyses. Fetal gender was identified by using PCR (Tunster, 2017).

To analyze the effects of ME on offspring performance, the above mouse study was repeated and dams were allowed to give live birth. At birth, the litter sizes were normalized to 6. One male and one female weanling mice per litter were randomly selected and subjected to an acute exercise (n = 5 per group). Another set of male and female weanling mice were euthanized for muscle tissue collection (n = 6 per group). The remaining females and males (n = 6 per treatment) were weaned to a high obesogenic diet (60% energy from fat, Research Diets) to mimic a post-weaning obese environment. After 2 months of high fat diet (HFD) challenge, these mice were anesthetized for further analyses. For testing endurance exercise capacity, additional female and male mice fed a HFD for 2 months were subjected to an acute treadmill exercise (n = 4 per group). Mice were housed under a 12-h light/dark cycle at 22°C with food and water provided *ad libitum*.

For apelin administration, [Pyr1]apelin-13 (AAPPTec, Louisville, KY, USA) or PBS was injected daily at 0.5 mmol/kg/day (i.p) from E1.5 to E16.5 (Vinel et al., 2018). Apelin administered dams were euthanized and the fetuses were harvested 2 days after the last apelin injection (E18.5). The physiological changes of both maternal exercise and apelin administration studies have been reported in our previous studies (Son et al., 2019b, 2020).

The gastrocnemius muscle tissues, composed of mixed fibers, from offspring mice were utilized for biochemical analyses, including RT-PCR and western blotting. The soleus, type I fiber dominant muscle, was used for morphometrical analyses. Additionally, muscle fiber

compositions were qualified in the central (enriched with oxidative fibers) and lateral (enriched with glycolytic fibers) portion of TA muscle, including I, IIa, IIb, and IIx. All animal procedures were approved by the Institute of Animal Care and Use Committees (IACUC) at the Washington State University.

Primary cell culture—To generate apelin receptor (*Apj*) knockdown (KD) mice, *Apj* floxed mice (Sharma et al., 2017) were crossbred with *β-actin*[Cre]. Primary myogenic cells were isolated from hindlimb muscle of young *β-actin*[Cre]/*Apj*[flox/+] mice. Briefly, hindlimb muscle was collected, washed with PBS, and minced. Then, minced tissue was digested in minimal media with 0.75 units/mL collagenase D (StemCell Technologies, Inc., Vancouver, BC, Canada) for 35 min at 37°C. Cells were collected following centrifugation at $500 \times g$ for 15 min after passing through 100 and 40 μm filter strainers. Cells were seeded in F12 medium containing 20% FBS and 10 ng/mL of FGF2. To induce myogenic differentiation, cells were resuspended into the DMEM with 2% horse serum and 1% antibiotics (Fu et al., 2015).

METHOD DETAILS

Treadmill exercise protocol—For chronic treadmill exercise training, pregnant mice were exercised daily at the same time following the principles of progressive loading in intensity and duration, as described in a previous study (Son et al., 2019b). Briefly, female mice were subjected to flat degree of treadmill adaptation at 10 m/min for 10 min, 3 times/ week, for a week before mating for adapting to a treadmill environment. Then, pregnant mice were subjected to treadmill exercise training every morning for an hour in accordance with exercise regimen as follows: warming up (5 m/min for 10 min), main exercise (10 to 14 m/min for 40 min) and cooling down (5 m/min for 10 min). The intensity of exercise consisted of three different time frames: E1.5 to E7.5 (40%), E8.5 to E14.5 (65%) and E15.5 to E16.5 (50%) of the VO_2 max (Zavorsky and Longo, 2011). For a single bout of exercise at weaning, one female and one male offspring mice per litter were subjected to an adaptation for treadmill exercise at 10 m/min, 3 times for one week as previously reported (Son et al., 2019b). Then, mice were subjected to 25 degree inclined treadmill running exercise along with the measurement of respiratory metabolic ability using a treadmill respiratory measurement system (Oxymax fast 4 lane modular treadmill system, Columbus Instruments, Columbus, OH, USA). The exercise started at 5 m/min for 5 min, and speed increased every 5 min (5.0, 8.0, 12.0, 15.0, 17.2, and 21.8 m/min) until 30 min.

Forelimb grip strength test—For forelimb grip strength measurement, a grip strength meter was used (Columbus Instruments). Maximal forelimb grip strength was determined by using a maximal value during ten repetition maximum (RM) measurements, and endurance grip strength was assessed by sequential ten RM measurements, as described in a previous report (Son et al., 2019b).

Transmission electron microscopic analysis—Transmission electron microscopic examination of muscle structure was performed as previously described (Yang et al., 2016).

Gas chromatography-mass spectrometry (GC-MS)—The metabolites were extracted from homogenized frozen muscle tissues using lysis buffer (20 mM Tris-HCL, 4.0 mM EDTA, 20 mM NaCl, 1% SDS), and used for GC-MS analysis (Zhang et al., 2019).

RNA sequencing—Alternative polyadenylation with whole transcriptome termini site sequencing (WTTS-seq) was conducted as previously reported (Son et al., 2020; Zhou et al., 2016). Briefly, we generated 72.6 million raw reads from clusters of Poly(A) sites (PACs). After trimming, 70.5 million (97%) reads remained, and 53.1 million reads (73.05%) were mapped to reference genome (Mus_musculus.GRCm38.fa). Then, differential expressed gene (DEG) and gene ontology (GO) analyses were performed. Raw data for Figure 5 are included in Table S2.

Quantitative RT-PCR analysis—Total RNA was extracted from fetal skeletal muscle and offspring gastrocnemius muscle using TRIzol reagent (Invitrogen, Grand Island, NY, USA) and five-hundred nanogram of total RNA was reverse transcribed with an iScript™ cDNA Synthesis Kit (Bio-Rad, Hercules, CA, USA). Quantitative RT-PCR reactions were conducted using SsoAdvanced™ Universal SYBR® Green Supermix (Bio-Rad). 18S rRNA was used for normalization and relative mRNA was calculated by a comparative method ($2^{-\triangle \triangle Ct}$) as previously described (Son et al., 2019b). Primer sequences are listed in Table S1.

Mitochondrial DNA content—The copy number of mitochondrial DNA (mtDNA) was quantified by measuring NADH dehydrogenase subunit 1(*Nd1*) and normalized to the nuclear DNA lipoprotein lipase (*Lpl*) gene (genomic DNA) using RT-PCR (Maurya et al., 2018). The primers were mtDNA *Nd1* (*mNd1*) forward, 5′-CACTATTCGGAGCTTTACG-3′; *mNd1* reverse, 5′-TGTTTCTGCTAGGGTTGA-3′; *Lpl* forward, 5′-GAAAGGGCTCTGCCTGAGTT-3′; and *Lpl* reverse, 5′-TAGGGCATCTGAGAGCGAGT-3′.

Methylated DNA immunoprecipitation (MeDIP) PCR—Genomic DNA (20 μg) was isolated from gastrocnemius muscle using lysis buffer (10 mM Tris-HCl, 1.0 mM EDTA, 20 mM NaCl, 1% SDS) with 20 mg/ml proteinase K (VWR International, Radnor, PA, USA). DNA diluted with TE buffer was sonicated and denatured. This DNA (2 μg) was incubated with IgG, 5hmC, or 5mC antibodies in IP buffer (10 mM Na-phosphate, 140 mM NaCl, 0.05% Triton X-100). Immunoprecipitation was performed using EcoMag™ Protein A Magnetic Particles (#MJA-102, Bioclone Inc., San Diego, CA, USA) and then used for quantitative RT-PCR utilizing SsoAdvanced™ Universal SYBR® Green Supermix (Bio-Rad). IgG was used for normalization as previously described (Yang et al., 2016) and sequences of primers are listed in Table S1.

Western blot analysis—Protein extracts were obtained from gastrocnemius muscles using lysis buffer (100 mM Tris-HCl, pH 6.8, 2.0% SDS, 20% glycerol, 0.02% bromophenol blue, 5% 2-mercaptoethanol, 100 mM NaF and 1 mM Na$_3$VO$_4$) and the protein concentration of lysates was determined using a BCA Protein Assay Kit II (BioVision, Milpitas, CA, USA). Primary and secondary antibodies used in this study are listed in Key Resources Table. Target proteins were detected using an Odyssey Infrared Imaging System

(LI-COR Biosciences) as previously described (Son et al., 2019b). All uncropped images are listed in Data S1.

Histological analysis—For immunocytochemical (ICC) staining, skeletal muscles were removed and embedded in paraffin following 24 h fixation with 4% paraformaldehyde. Sections (5 μm thickness) of soleus and tibialis anterior muscles were prepared for CD31 (dilution 1:50) ICC staining as previously described (Son et al., 2017). For the secondary antibody, anti-rabbit IgG Alexa 555 (dilution 1:200) was used.

For staining specific muscle fiber types, fresh tissues were embedded in OCT compound (Thermo 6502, Thermo Fisher Scientific, Waltham, MA, USA), and sections (10 μm thickness) were utilized for staining using anti-myosin heavy chain (MHC) I, anti-MHC IIa, and anti-MHC IIb mouse monoclonal antibodies as primary antibodies. For the secondary antibodies, goat anti-mouse IgG2b Alexa 488, goat anti-mouse IgG1 Alexa 555, and goat anti-mouse IgM Alexa 350 antibodies were purchased from ThermoFisher Scientific. Images were generated by the EVOS® XL Core Imaging System (Mil Creek, WA, USA). Then, the cross-sectional areas were measured in ImageJ (NIH) according to the previous report (Son et al., 2020).

QUANTIFICATION AND STATISTICAL ANALYSIS

Data were visualized using Prism, Ver. 7 (GraphPad Software, San Diego, CA, USA) and presented as mean ± s.e.m. Statistical significance was defined as $p < 0.05$, which was determined by Student t test or two-way repeated-measures ANOVA with Tukey's test (SAS Institute Inc., Cary, NC, USA). The number of samples and p values for each measurement is indicated in the figure legends. For WTTS-seq, R Statistics and SPSS Statistics ver.21 (IBM Corp., Armonk, NY, USA) were further used for principal component analyses (PCA), differential expressed genes (DEGs), gene ontology (GO), and hierarchical cluster analysis.

Supplementary Material

Refer to Web version on PubMed Central for supplementary material.

ACKNOWLEDGMENTS

REFERENCES

Archer E, Lavie CJ, McDonald SM, Thomas DM, Hébert JR, Taverno Ross SE, McIver KL, Malina RM, and Blair SN (2013). Maternal inactivity: 45-year trends in mothers' use of time. Mayo Clin. Proc 88, 1368–1377. [PubMed: 24290110]

Attané C, Foussal C, Le Gonidec S, Benani A, Daviaud D, Wanecq E, Guzmán-Ruiz R, Dray C, Bezaire V, Rancoule C, et al. (2012). Apelin treatment increases complete Fatty Acid oxidation, mitochondrial oxidative capacity, and biogenesis in muscle of insulin-resistant mice. Diabetes 61, 310–320. [PubMed: 22210322]

Barakat R, Perales M, Garatachea N, Ruiz JR, and Lucia A (2015). Exercise during pregnancy. A narrative review asking: what do we know? Br. J. Sports Med 49, 1377–1381. [PubMed: 26135742]

Cantó C, Jiang LQ, Deshmukh AS, Mataki C, Coste A, Lagouge M, Zierath JR, and Auwerx J (2010). Interdependence of AMPK and SIRT1 for metabolic adaptation to fasting and exercise in skeletal muscle. Cell Metab. 11, 213–219. [PubMed: 20197054]

Chen M, Feng HZ, Gupta D, Kelleher J, Dickerson KE, Wang J, Hunt D, Jou W, Gavrilova O, Jin JP, and Weinstein LS (2009). G(s)alpha deficiency in skeletal muscle leads to reduced muscle mass, fiber-type switching, and glucose intolerance without insulin resistance or deficiency. Am. J. Physiol. Cell Physiol 296, C930–C940. [PubMed: 19158402]

Chen X, Luo X, Chen D, Yu B, He J, and Huang Z (2020). Arginine promotes porcine type I muscle fibres formation through improvement of mitochondrial biogenesis. Br. J. Nutr 123, 499–507. [PubMed: 31779731]

Clapp JF (2006). Influence of endurance exercise and diet on human placental development and fetal growth. Placenta 27, 527–534. [PubMed: 16165206]

Davenport MH, Meah VL, Ruchat SM, Davies GA, Skow RJ, Barrowman N, Adamo KB, Poitras VJ, Gray CE, Jaramillo Garcia A, et al. (2018). Impact of prenatal exercise on neonatal and childhood outcomes: a systematic review and meta-analysis. Br. J. Sports Med 52, 1386–1396. [PubMed: 30337465]

de Meester C, Timmermans AD, Balteau M, Ginion A, Roelants V, Noppe G, Porporato PE, Sonveaux P, Viollet B, Sakamoto K, et al. (2014). Role of AMP-activated protein kinase in regulating hypoxic survival and proliferation of mesenchymal stem cells. Cardiovasc. Res 101, 20–29. [PubMed: 24104879]

Dray C, Knauf C, Daviaud D, Waget A, Boucher J, Buléon M, Cani PD, Attané C, Guigné C, Carpéné C, et al. (2008). Apelin stimulates glucose utilization in normal and obese insulin-resistant mice. Cell Metab. 8, 437–445. [PubMed: 19046574]

Dzeja PP, Chung S, Faustino RS, Behfar A, and Terzic A (2011). Developmental enhancement of adenylate kinase-AMPK metabolic signaling axis supports stem cell cardiac differentiation. PLoS One 6, e19300.

Folmes CD, Nelson TJ, Martinez-Fernandez A, Arrell DK, Lindor JZ, Dzeja PP, Ikeda Y, Perez-Terzic C, and Terzic A (2011). Somatic oxidative bioenergetics transitions into pluripotency-dependent glycolysis to facilitate nuclear reprogramming. Cell Metab. 14, 264–271. [PubMed: 21803296]

Friedman JE (2018). Developmental Programming of Obesity and Diabetes in Mouse, Monkey, and Man in 2018: Where Are We Headed? Diabetes 67, 2137–2151. [PubMed: 30348820]

Frier BC, Williams DB, and Wright DC (2009). The effects of apelin treatment on skeletal muscle mitochondrial content. Am. J. Physiol. Regul. Integr. Comp. Comp. Physiol 297, R1761–R1768.

Frisbee JC, Lewis MT, and Wiseman RW (2019). Skeletal muscle performance in metabolic disease: Microvascular or mitochondrial limitation or both? Microcirculation 26, e12517.

Fu X, Zhu MJ, Dodson MV, and Du M (2015). AMP-activated protein kinase stimulates Warburg-like glycolysis and activation of satellite cells during muscle regeneration. J. Biol. Chem 290, 26445–26456. [PubMed: 26370082]

Fu X, Zhu M, Zhang S, Foretz M, Viollet B, and Du M (2016). Obesity Impairs Skeletal Muscle Regeneration Through Inhibition of AMPK. Diabetes 65, 188–200. [PubMed: 26384382]

Godfrey KM, Reynolds RM, Prescott SL, Nyirenda M, Jaddoe VW, Eriksson JG, and Broekman BF (2017). Influence of maternal obesity on the long-term health of offspring. Lancet Diabetes Endocrinol. 5, 53–64. [PubMed: 27743978]

Granata C, Oliveira RSF, Little JP, Renner K, and Bishop DJ (2016). Mitochondrial adaptations to high-volume exercise training are rapidly reversed after a reduction in training volume in human skeletal muscle. FASEB J. 30, 3413–3423. [PubMed: 27402675]

Gustafsson MK, Stafne SN, Romundstad PR, Mørkved S, Salvesen K, and Helvik AS (2016). The effects of an exercise programme during pregnancy on health-related quality of life in pregnant women: a Norwegian randomised controlled trial. BJOG 123, 1152–1160. [PubMed: 26265465]

Habegger KM, Hoffman NJ, Ridenour CM, Brozinick JT, and Elmendorf JS (2012). AMPK enhances insulin-stimulated GLUT4 regulation via lowering membrane cholesterol. Endocrinology 153, 2130–2141. [PubMed: 22434076]

Hardie DG (2007a). AMP-activated/SNF1 protein kinases: conserved guardians of cellular energy. Nat. Rev. Mol. Cell Biol 8, 774–785. [PubMed: 17712357]

Hardie DG (2007b). Biochemistry. Balancing cellular energy. Science 315, 1671–1672. [PubMed: 17379794]

Heo JW, No MH, Park DH, Kang JH, Seo DY, Han J, Neufer PD, and Kwak HB (2017). Effects of exercise on obesity-induced mitochondrial dysfunction in skeletal muscle. Korean J. Physiol. Pharmacol 21, 567–577. [PubMed: 29200899]

Hesselink MKC, Schrauwen-Hinderling V, and Schrauwen P (2016). Skeletal muscle mitochondria as a target to prevent or treat type 2 diabetes mellitus. Nat. Rev. Endocrinol 12, 633–645. [PubMed: 27448057]

Higuchi K, Masaki T, Gotoh K, Chiba S, Katsuragi I, Tanaka K, Kakuma T, and Yoshimatsu H (2007). Apelin, an APJ receptor ligand, regulates body adiposity and favors the messenger ribonucleic acid expression of uncoupling proteins in mice. Endocrinology 148, 2690–2697. [PubMed: 17347313]

Ho L, van Dijk M, Chye STJ, Messerschmidt DM, Chng SC, Ong S, Yi LK, Boussata S, Goh GH, Afink GB, et al. (2017). ELABELA deficiency promotes preeclampsia and cardiovascular malformations in mice. Science 357, 707–713. [PubMed: 28663440]

Hopkins SA, and Cutfield WS (2011). Exercise in pregnancy: weighing up the long-term impact on the next generation. Exerc. Sport Sci. Rev 39, 120–127. [PubMed: 21519301]

Janssen I, Heymsfield SB, Wang ZM, and Ross R (2000). Skeletal muscle mass and distribution in 468 men and women aged 18–88 yr. J. Appl. Physiol 89, 81–88. [PubMed: 10904038]

Kalinkovich A, and Livshits G (2017). Sarcopenic obesity or obese sarcopeia: A cross talk between age-associated adipose tissue and skeletal muscle inflammation as a main mechanism of the pathogenesis. Ageing Res. Rev 35, 200–221. [PubMed: 27702700]

Kang H, Viollet B, and Wu D (2013). Genetic deletion of catalytic subunits of AMP-activated protein kinase increases osteoclasts and reduces bone mass in young adult mice. J. Biol. Chem 288, 12187–12196. [PubMed: 23486478]

Kim TN, Park MS, Yang SJ, Yoo HJ, Kang HJ, Song W, Seo JA, Kim SG, Kim NH, Baik SH, et al. (2010). Prevalence and determinant factors of sarcopenia in patients with type 2 diabetes: the Korean Sarcopenic Obesity Study (KSOS). Diabetes Care 33, 1497–1499. [PubMed: 20413515]

Laker RC, Lillard TS, Okutsu M, Zhang M, Hoehn KL, Connelly JJ, and Yan Z (2014). Exercise prevents maternal high-fat diet-induced hypermethylation of the Pgc-1α gene and age-dependent metabolic dysfunction in the offspring. Diabetes 63, 1605–1611. [PubMed: 24430439]

Lantier L, Fentz J, Mounier R, Leclerc J, Treebak JT, Pehmøller C, Sanz N, Sakakibara I, Saint-Amand E, Rimbaud S, et al. (2014). AMPK controls exercise endurance, mitochondrial oxidative capacity, and skeletal muscle integrity. FASEB J. 28, 3211–3224. [PubMed: 24652947]

Lin J, Wu H, Tarr PT, Zhang CY, Wu Z, Boss O, Michael LF, Puigserver P, Isotani E, Olson EN, et al. (2002). Transcriptional co-activator PGC-1 alpha drives the formation of slow-twitch muscle fibres. Nature 418, 797–801. [PubMed: 12181572]

Loprinzi PD, and Frith E (2019). Protective and therapeutic effects of exercise on stress-induced memory impairment. J Physiol Sci 69, 1–12.

Mangwiro YTM, Cuffe JSM, Briffa JF, Mahizir D, Anevska K, Jefferies AJ, Hosseini S, Romano T, Moritz KM, and Wlodek ME (2018). Maternal exercise in rats upregulates the placental insulin-like growth factor system with diet- and sex-specific responses: minimal effects in mothers born growth restricted. J. Comp. Physiol 596, 5947–5964.

Maurya SK, Herrera JL, Sahoo SK, Reis FCG, Vega RB, Kelly DP, and Periasamy M (2018). Sarcolipin Signaling Promotes Mitochondrial Biogenesis and Oxidative Metabolism in Skeletal Muscle. Cell Rep. 24, 2919–2931. [PubMed: 30208317]

McCurdy CE, Bishop JM, Williams SM, Grayson BE, Smith MS, Friedman JE, and Grove KL (2009). Maternal high-fat diet triggers lipotoxicity in the fetal livers of nonhuman primates. J. Clin. Invest 119, 323–335. [PubMed: 19147984]

McPherron AC, Lawler AM, and Lee SJ (1997). Regulation of skeletal muscle mass in mice by a new TGF-beta superfamily member. Nature 387, 83–90. [PubMed: 9139826]

Menshikova EV, Ritov VB, Ferrell RE, Azuma K, Goodpaster BH, and Kelley DE (2007). Characteristics of skeletal muscle mitochondrial biogenesis induced by moderate-intensity exercise and weight loss in obesity. J. Appl. Comp. Physiol 103, 21–27.

Menzies KJ, Singh K, Saleem A, and Hood DA (2013). Sirtuin 1-mediated effects of exercise and resveratrol on mitochondrial biogenesis. J. Biol. Chem 288, 6968–6979. [PubMed: 23329826]

Misu H, Takayama H, Saito Y, Mita Y, Kikuchi A, Ishii KA, Chikamoto K, Kanamori T, Tajima N, Lan F, et al. (2017). Deficiency of the hepatokine selenoprotein P increases responsiveness to exercise in mice through upregulation of reactive oxygen species and AMP-activated protein kinase in muscle. Nat. Med 23, 508–516. [PubMed: 28263310]

Moyer C, Reoyo OR, and May L (2016). The Influence of Prenatal Exercise on Offspring Health: A Review. Clin. Med. Insights Womens Health 9, 37–42. [PubMed: 27777506]

Nascimento SL, Surita FG, and Cecatti JG (2012). Physical exercise during pregnancy: a systematic review. Curr. Opin. Obstet. Gynecol 24, 387–394. [PubMed: 23014142]

Neeland IJ, Turer AT, Ayers CR, Powell-Wiley TM, Vega GL, Farzaneh-Far R, Grundy SM, Khera A, McGuire DK, and de Lemos JA (2012). Dysfunctional adiposity and the risk of prediabetes and type 2 diabetes in obese adults. JAMA 308, 1150–1159. [PubMed: 22990274]

Oberbach A, Bossenz Y, Lehmann S, Niebauer J, Adams V, Paschke R, Schön MR, Blüher M, and Punkt K (2006). Altered fiber distribution and fiber-specific glycolytic and oxidative enzyme activity in skeletal muscle of patients with type 2 diabetes. Diabetes Care 29, 895–900. [PubMed: 16567834]

Ochocki JD, and Simon MC (2013). Nutrient-sensing pathways and metabolic regulation in stem cells. J. Cell Biol 203, 23–33. [PubMed: 24127214]

Otero-Díaz B, Rodríguez-Flores M, Sánchez-Muñoz V, Monraz-Preciado F, Ordoñez-Ortega S, Becerril-Elias V, Baay-Guzmán G, Obando-Monge R, García-García E, Palacios-González B, et al. (2018). Exercise Induces White Adipose Tissue Browning Across the Weight Spectrum in Humans. Front. Comp. Physiol 9, 1781.

Palacios OM, Carmona JJ, Michan S, Chen KY, Manabe Y, Ward JL 3rd, Goodyear LJ, and Tong Q (2009). Diet and exercise signals regulate SIRT3 and activate AMPK and PGC-1alpha in skeletal muscle. Aging (Albany NY) 1, 771–783. [PubMed: 20157566]

Patki G, et al. (2014). Moderate treadmill exercise rescues anxiety and depression-like behavior as well as memory posttraumatic stress disorder. Physiol Behav 130, 47–53. [PubMed: 24657739]

Peres Valgas da Silva C, Hernández-Saavedra D, White JD, and Stanford KI (2019). Cold and Exercise: Therapeutic Tools to Activate Brown Adipose Tissue and Combat Obesity. Biology (Basel) 8, 9.

Power ML, and Schulkin J (2013). Maternal regulation of offspring development in mammals is an ancient adaptation tied to lactation. Appl. Transl. Genomics 2, 55–63.

Richter EA, and Hargreaves M (2013). Exercise, GLUT4, and skeletal muscle glucose uptake. Physiol. Rev 93, 993–1017. [PubMed: 23899560]

Roy B, Curtis ME, Fears LS, Nahashon SN, and Fentress HM (2016). Molecular Mechanisms of Obesity-Induced Osteoporosis and Muscle Atrophy. Front. Comp. Physiol 7, 439.

Ruas JL, White JP, Rao RR, Kleiner S, Brannan KT, Harrison BC, Greene NP, Wu J, Estall JL, Irving BA, et al. (2012). A PGC-1α isoform induced by resistance training regulates skeletal muscle hypertrophy. Cell 151, 1319–1331. [PubMed: 23217713]

Sandri M, Lin J, Handschin C, Yang W, Arany ZP, Lecker SH, Goldberg AL, and Spiegelman BM (2006). PGC-1alpha protects skeletal muscle from atrophy by suppressing FoxO3 action and atrophy-specific gene transcription. Proc. Natl. Acad. Sci. USA 103, 16260–16265. [PubMed: 17053067]

Seo JH (2018). Treadmill exercise alleviates stress-induced anxiety-like behaviors in rats. J Exerc Rehabil 14 (5), 724–730. [PubMed: 30443516]

Shah M, Kola B, Bataveljic A, Arnett TR, Viollet B, Saxon L, Korbonits M, and Chenu C (2010). AMP-activated protein kinase (AMPK) activation regulates in vitro bone formation and bone mass. Bone 47, 309–319. [PubMed: 20399918]

Sharma B, Ho L, Ford GH, Chen HI, Goldstone AB, Woo YJ, Quertermous T, Reversade B, and Red-Horse K (2017). Alternative Progenitor Cells Compensate to Rebuild the Coronary Vasculature in Elabela- and Apj-Deficient Hearts. Dev. Cell 42, 655–666.e3. [PubMed: 28890073]

Son JS, Kim HJ, Son Y, Lee H, Chae SA, Seong JK, and Song W (2017). Effects of exercise-induced apelin levels on skeletal muscle and their capillarization in type 2 diabetic rats. Muscle Nerve 56, 1155–1163. [PubMed: 28164323]

Son JS, Chae SA, Park BI, Du M, and Song W (2019a). Plasma apelin levels in overweight/obese adults following a single bout of exhaustive exercise: A preliminary cross-sectional study. Endocrinol. Diabetes Nutr 66, 278–290. [PubMed: 30827910]

Son JS, Liu X, Tian Q, Zhao L, Chen Y, Hu Y, Chae SA, de Avila JM, Zhu MJ, and Du M (2019b). Exercise prevents the adverse effects of maternal obesity on placental vascularization and fetal growth. J. Comp. Physiol 597, 3333–3347.

Son JS, Zhao L, Chen Y, Chen K, Chae SA, de Avila JM, Wang H, Zhu MJ, Jiang Z, and Du M (2020). Maternal exercise via exerkine apelin enhances brown adipogenesis and prevents metabolic dysfunction in offspring mice. Sci. Adv 6, eaaz0359.

Stanford KI, Lee MY, Getchell KM, So K, Hirshman MF, and Goodyear LJ (2015). Exercise before and during pregnancy prevents the deleterious effects of maternal high-fat feeding on metabolic health of male offspring. Diabetes 64, 427–433. [PubMed: 25204976]

Stanford KI, Takahashi H, So K, Alves-Wagner AB, Prince NB, Lehnig AC, Getchell KM, Lee MY, Hirshman MF, and Goodyear LJ (2017). Maternal Exercise Improves Glucose Tolerance in Female Offspring. Diabetes 66, 2124–2136. [PubMed: 28572303]

Than A, He HL, Chua SH, Xu D, Sun L, Leow MK, and Chen P (2015). Apelin Enhances Brown Adipogenesis and Browning of White Adipocytes. J. Biol. Chem 290, 14679–14691. [PubMed: 25931124]

Theilen NT, Kunkel GH, and Tyagi SC (2017). The Role of Exercise and TFAM in Preventing Skeletal Muscle Atrophy. J. Cell. Comp. Physiol 232, 2348–2358.

Tong JF, Yan X, Zhao JX, Zhu MJ, Nathanielsz PW, and Du M (2011b). Metformin mitigates the impaired development of skeletal muscle in the offspring of obese mice. Nutr. Diabetes 1, e7. [PubMed: 23449382]

Tunster SJ (2017). Genetic sex determination of mice by simplex PCR. Biol. Sex Differ 8, 31. [PubMed: 29041956]

Vazquez-Martin A, Corominas-Faja B, Cufi S, Vellon L, Oliveras-Ferraros C, Menendez OJ, Joven J, Lupu R, and Menendez JA (2013). The mitochondrial H(+)-ATP synthase and the lipogenic switch: new core components of metabolic reprogramming in induced pluripotent stem (iPS) cells. Cell Cycle 12, 207–218. [PubMed: 23287468]

Vinel C, Lukjanenko L, Batut A, Deleruyelle S, Pradére JP, Le Gonidec S, Dortignac A, Geoffre N, Pereira O, Karaz S, et al. (2018). The exerkine apelin reverses age-associated sarcopenia. Nat. Med 24, 1360–1371. [PubMed: 30061698]

Wende AR, Schaeffer PJ, Parker GJ, Zechner C, Han DH, Chen MM, Hancock CR, Lehman JJ, Huss JM, McClain DA, et al. (2007). A role for the transcriptional coactivator PGC-1alpha in muscle refueling. J. Biol. Chem 282, 36642–36651. [PubMed: 17932032]

White JP, Wrann CD, Rao RR, Nair SK, Jedrychowski MP, You JS, Martínez-Redondo V, Gygi SP, Ruas JL, Hornberger TA, et al. (2014). G protein-coupled receptor 56 regulates mechanical overload-induced muscle hypertrophy. Proc. Natl. Acad. Sci. USA 111, 15756–15761. [PubMed: 25336758]

Yan X, Zhu MJ, Xu W, Tong JF, Ford SP, Nathanielsz PW, and Du M (2010). Up-regulation of Toll-like receptor 4/nuclear factor-kappaB signaling is associated with enhanced adipogenesis and insulin resistance in fetal skeletal muscle of obese sheep at late gestation. Endocrinology 151, 380–387. [PubMed: 19887565]

Yang Q, Liang X, Sun X, Zhang L, Fu X, Rogers CJ, Berim A, Zhang S, Wang S, Wang B, et al. (2016). AMPK/a-Ketoglutarate Axis Dynamically Mediates DNA Demethylation in the Prdm16 Promoter and Brown Adipogenesis. Cell Metab. 24, 542–554. [PubMed: 27641099]

Yu WM, Liu X, Shen J, Jovanovic O, Pohl EE, Gerson SL, Finkel T, Broxmeyer HE, and Qu CK (2013). Metabolic regulation by the mitochondrial phosphatase PTPMT1 is required for hematopoietic stem cell differentiation. Cell Stem Cell 12, 62–74. [PubMed: 23290137]

Zavorsky GS, and Longo LD (2011). Exercise guidelines in pregnancy: new perspectives. Sports Med. 41, 345–360. [PubMed: 21510713]

Zhang S, Wang H, and Zhu MJ (2019). A sensitive GC/MS detection method for analyzing microbial metabolites short chain fatty acids in fecal and serum samples. Talanta 196, 249–254. [PubMed: 30683360]

Zhao J, Yue W, Zhu MJ, Sreejayan N, and Du M (2010). AMP-activated protein kinase (AMPK) cross-talks with canonical Wnt signaling via phosphorylation of beta-catenin at Ser 552. Biochem. Biophys. Res. Commun 395, 146–151. [PubMed: 20361929]

Zhao JX, Yue WF, Zhu MJ, and Du M (2011). AMP-activated protein kinase regulates beta-catenin transcription via histone deacetylase 5. J. Biol. Chem 286, 16426–16434. [PubMed: 21454484]

Zhou X, Li R, Michal JJ, Wu XL, Liu Z, Zhao H, Xia Y, Du W, Wildung MR, Pouchnik DJ, et al. (2016). Accurate Profiling of Gene Expression and Alternative Polyadenylation with Whole Transcriptome Termini Site Sequencing (WTTS-Seq). Genetics 203, 683–697. [PubMed: 27098915]

Zhu MJ, Han B, Tong J, Ma C, Kimzey JM, Underwood KR, Xiao Y, Hess BW, Ford SP, Nathanielsz PW, and Du M (2008). AMP-activated protein kinase signalling pathways are down regulated and skeletal muscle development impaired in fetuses of obese, over-nourished sheep. J. Comp. Physiol 586, 2651–2664.

Highlights

- Maternal exercise increases oxidative muscle fibers and endurance in offspring

- Maternal exercise elevates apelin signaling to facilitate fetal muscle development

- Maternal exercise enhances *Ppargc1a* expression and mitochondriogenesis in fetal muscle

- Apelin mirrors beneficial effects of exercise on fetal muscle development
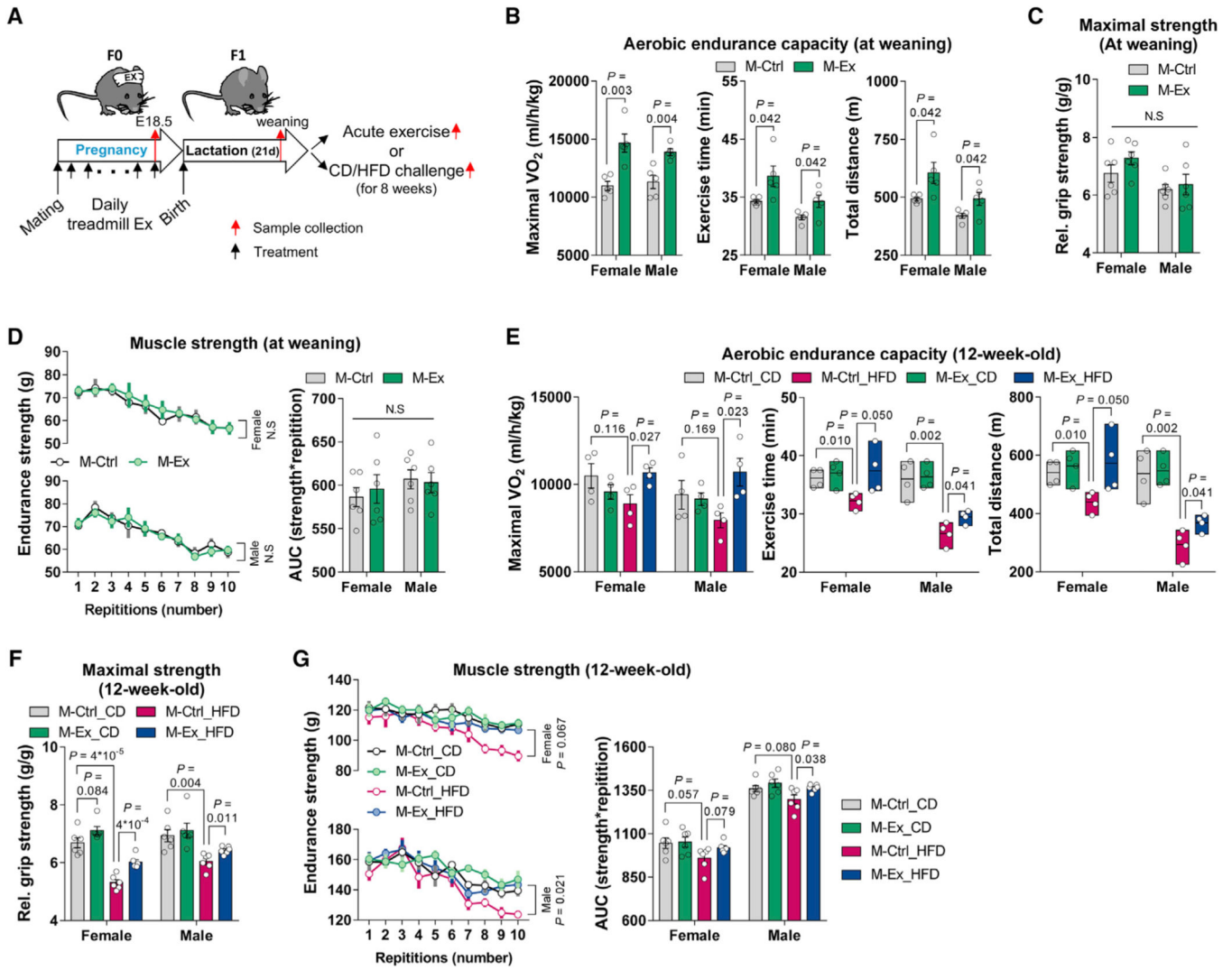
Figure 1. Maternal Exercise Enhances Adaptation to Endurance Training of Offspring Mice

Endurance capacity was assessed following a single bout of exercise in weanling and control/high-fat diet (CD/HFD)-challenged offspring, and the programming effect was demonstrated after CD/HFD challenge.

(A) A schematic diagram.

(B and E) Endurance capacity measurements following an acute exercise in the M-Ctrl and M-Ex weanling (B; n = 5/group) and CD/HFD-challenged (E; n = 4/group) offspring.

(C, D, F, and G) Forelimb maximal strength and endurance strength at weaning (C and D) and after CD/HFD challenge (F and G) in the female and male M-Ctrl and M-Ex offspring (n = 6/group).

Data are mean ± SEM, and each dot represents one litter; two-sided p values by unpaired Student's t test (B–G) or two-way repeated-measures ANOVA followed by Tukey's test (D–G).
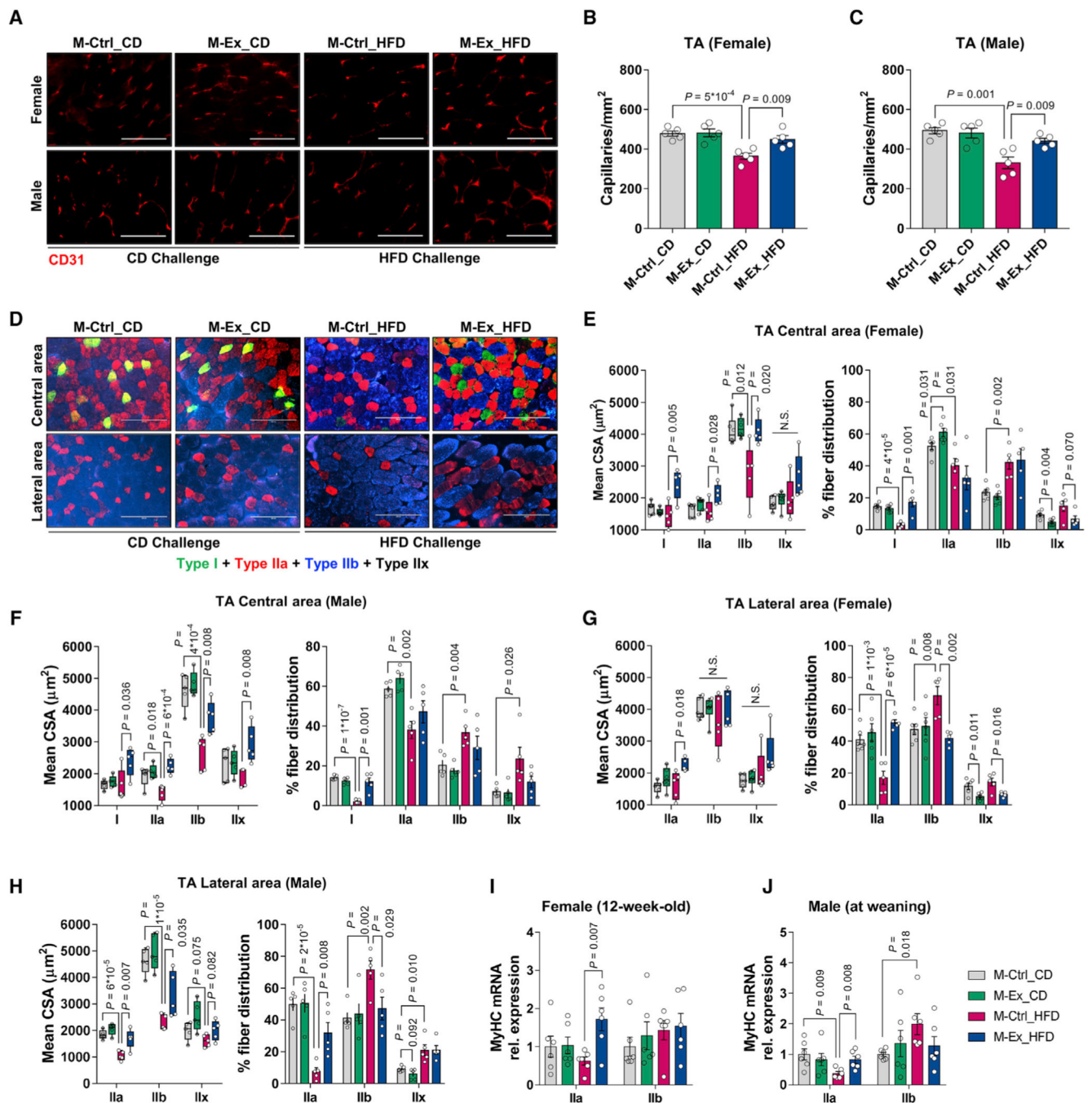
See also Figure S1.

Figure 2. Maternal Exercise Enhances the Proportion of Oxidative Fibers following CD/HFD Challenge

(A–C) Representative images of histological analysis (A) for measuring capillary density and their means (B and C) in the soleus and tibialis anterior (TA) muscles of female and male M-Ctrl and M-Ex offspring challenged with CD or HFD; scale bars represent 100 μm (n = 5 per group).

(D) Representative images of immunocytochemical staining (ICC) for myosin heavy chain type I and IIa, IIb, and IIx in the offspring following CD/HFD challenge; scale bars represent 200 μm.

(E–H) Mean cross-sectional areas (CSAs) and percent fiber distributions in the central area of TA after CD/ HFD challenge (E and F), or in the lateral area of TA after CD/HFD challenge (G and H); n = 5 per group.

(I) Gene expression of myosin heavy chains in the gastrocnemius muscle of CD/HFD-challenged offspring.

Data are mean ± SEM, and each dot represents one litter; two-way repeated-measures ANOVA followed by Tukey's test and two-sided p values by unpaired Student's t test (B, C, and E–J).
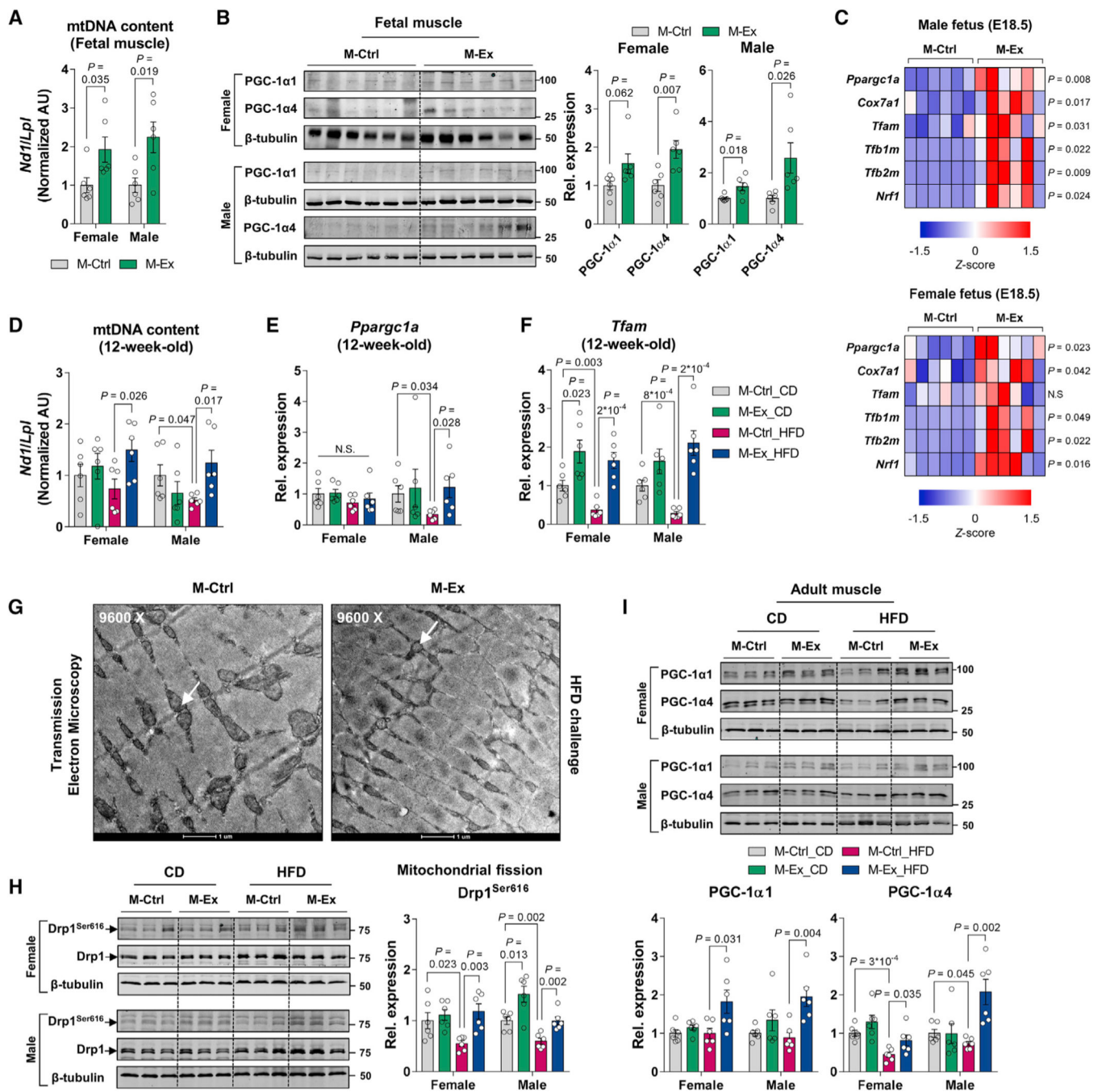
See also Figure S2.

Figure 3. Maternal Exercise Stimulates Mitochondrial Biogenesis and Oxidative Phosphorylation in the Skeletal Muscle of Offspring Mice at Weaning and following CD/HFD Challenge

(A) Mitochondrial DNA (mtDNA) content in the female and male fetuses (n = 6).

(B and C) Cropped western blots of PGC-1α1 and α4 protein levels (B) and mRNA expression of mitochondrial biogenic markers (C; n = 6).

(D–F) mtDNA content (D) and gene expressions of *Ppargc1a* (E) and *Tfam* (F) in the female and male offspring challenged with CD or HFD (n = 6).

(G) Representative images of transmission electron microscopy (TEM) in offspring M-Ctrl and M-Ex soleus muscle following HFD challenge. Scale bars represent 1 μm. Arrow, mitochondria.

(H and I) Cropped western blots of phosphorylated Drp1 protein levels (H) and PGC-1α1 and 4 isoform protein levels (I) in female and male offspring mice challenged with CD or HFD challenge (n = 6).

Data are mean ± SEM, and each dot represents one litter; two-sided p values by unpaired Student's t test (A–I) or two-way repeated-measures ANOVA followed by Tukey's test (D–I).
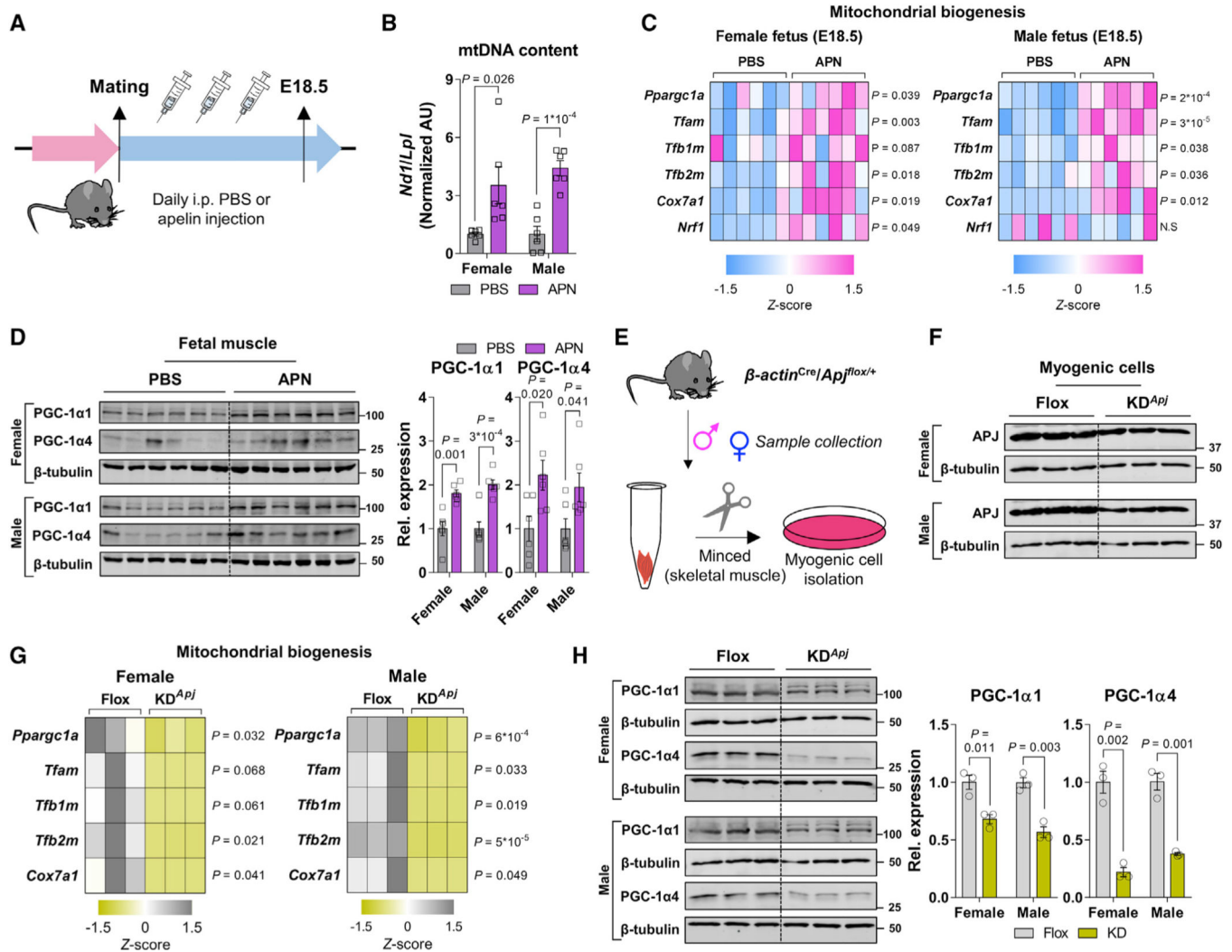
See also Figure S3.

Figure 4. Maternal Apelin/APJ Axis Mimics the Beneficial Effects of Maternal Exercise on Mitochondrial Biogenesis of Fetal Skeletal Muscle

(A) Design of apelin administration during pregnancy.

(B and C) mtDNA content (B) and gene expression related to mitochondrial biogenesis (C) in female and male fetal muscle at E18.5 (n = 6).

(D) Cropped western blots of PGC-1α1 and 4 isoform protein levels in female and male fetal muscles at E18.5 in response to maternal apelin administration during pregnancy (n = 6).

(E) Myogenic cell isolation from female and male *β-actin*Cre/*Apj*flox/+ weanling mice.

(F) Cropped western blots of knockdown (KD) of APJ protein levels in the isolated myogenic cells from female and male *β-actin*Cre/*Apj*flox/+ mice (KD^{Apj}; n = 3).

(G) Mitochondrial-biogenesis-related gene expression in the Flox and KD^{Apj} mice (n = 3).

(H) Cropped western blots of PGC-1α1 and 4 isoform protein levels in female and male Flox and KD^{Apj} (n = 3). Data are mean ± SEM, and each dot represents one litter; two-sided p values by unpaired Student's t test (A–H). See also Figure S4.
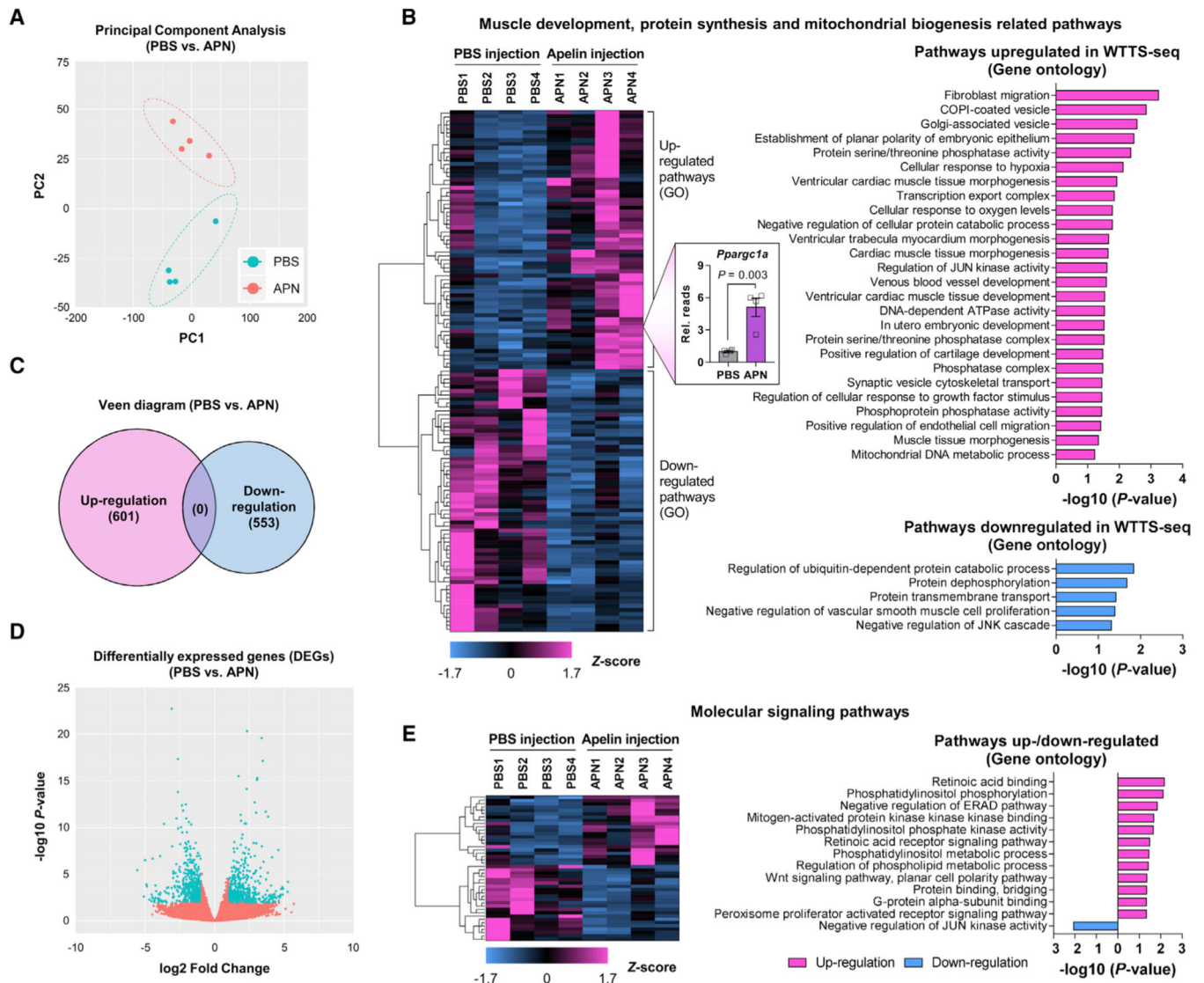
Figure 5. Whole-Transcriptome Termini Site Sequencing (WTTS-Seq) Analysis of Fetal Muscle following Maternal Apelin Administration

(A) Principal-component analysis of fetal muscle of PBS- and apelin-injected maternal mice (n = 4).

(B and E) Expression profile and Gene Ontology (GO) analysis of up-/downregulated genes related to muscle development and mitochondrial biogenesis (B) or molecular signaling pathways (E) (n = 4).

(C and D) Venn diagram (C) and volcano plot (D) of differentially expressed genes (DEGs) in the fetal muscle of PBS- or apelin-administered maternal mice (n = 4). The color scale shows *Z* score levels of each gene in a blue (low expression) to black to pink (high expression) scheme. PBS versus APN by two-tailed Student's t test (B and E).
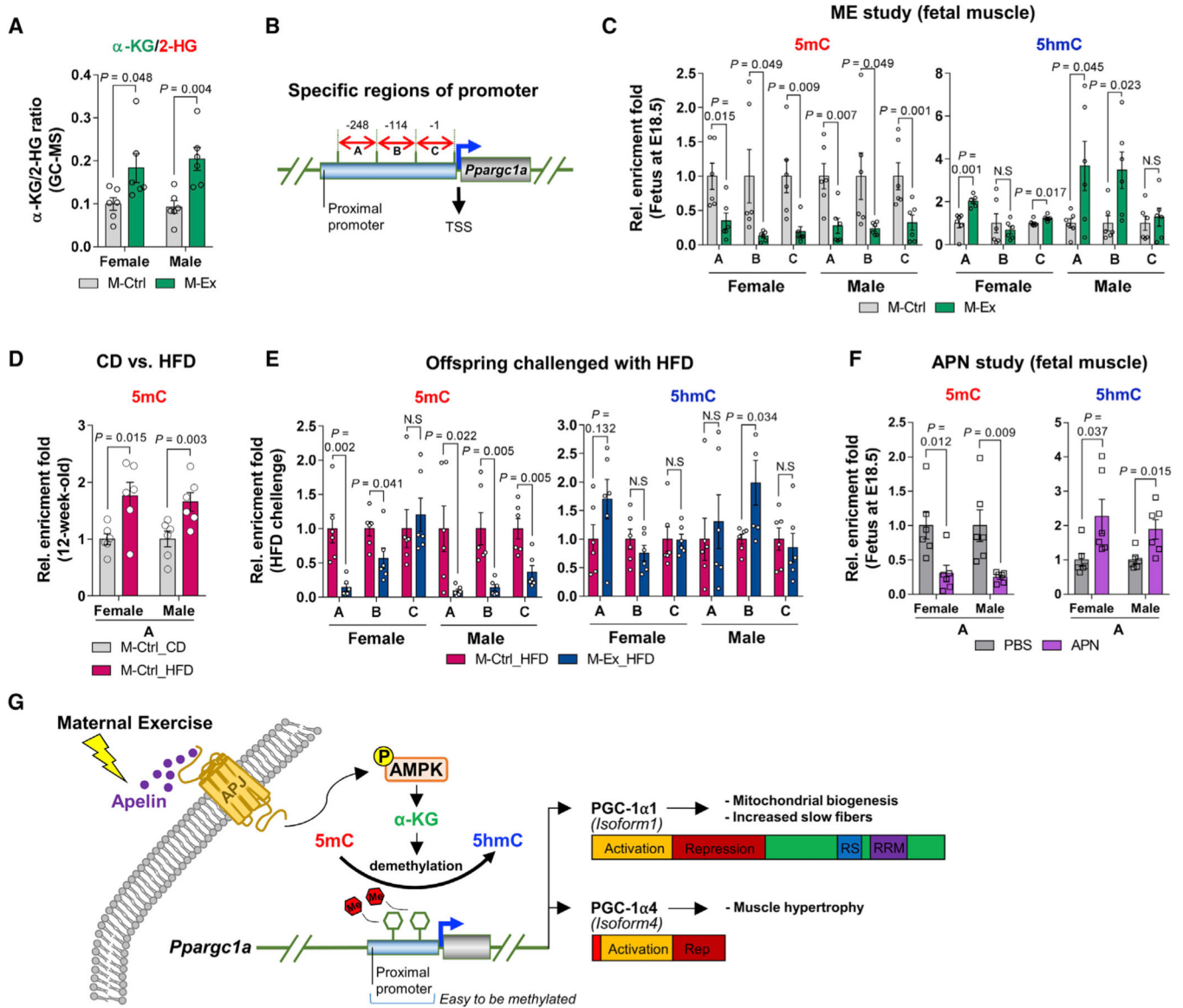
Figure 6. Maternal Exercise Stimulates DNA Hypomethylation of *Ppargc1a* Promoter

(A) The ratio of α-ketoglutarate (α-KG) to 2-hydroxyglutarate (2-HG) in fetal muscle at E18.5 (n = 6).

(B) Diagram showing three regions in the *Ppargc1a* proximal promoter.

(C) 5-methylcytosine (5mC) and 5-hydroxymethylcytosine (5hmC) enrichment fold of fetal skeletal muscle in response to maternal exercise (n = 6).

(D) 5mC enrichment fold in the gastrocnemius muscle of female and male M-Ctrl offspring challenged with CD or HFD (n = 6).

(E and F) 5mC and 5hmC enrichment fold of offspring gastrocnemius muscle after CD/HFD challenge in response to maternal exercise (E; n = 6) and fetal muscle following apelin administration during pregnancy (F; n = 6).

(G) A proposed mechanism of maternal-exercise-dependent AMPK/α-KG/*Ppargc1a* demethylation axis, stimulating mitochondrial biogenesis (PGC-1α1) and endurance performance.

Data are mean ± SEM, and each dot represents one litter; two-sided p values by unpaired Student's t test (A–F). See also Figure S5.

KEY RESOURCES TABLE

REAGENT or RESOURCE	SOURCE	IDENTIFIER
Antibodies		
Mouse monoclonal anti-PGC1a	Proteintech	Cat#66369-1-Ig; RRID: AB_2828002
Rabbit polyclonal anti-Apelin	Proteintech	Cat#11497-1-AP
Rabbit polyclonal anti-APJ	Proteintech	Car#20341-1-AP
Rabbit monoclonal anti-VDAC	Cell Signaling Technology	Cat#4661; RRID: AB_10557420
Rabbit monoclonal anti-Phospho-AMPKα (Thr172)	Cell Signaling Technology	Cat#2535; RRID: AB_331250
Mouse monoclonal anti-AMPKα	Cell Signaling Technology	Cat#2793; RRID: AB_915794
Rabbit polyclonal anti-Phospho-DRP1 (Ser616)	Cell Signaling Technology	Cat#3455; RRID: AB_2085352
Rabbit monoclonal anti-DRP1	Cell Signaling Technology	Cat#8570; RRID: AB_10950498
Mouse monoclonal anti-Cytochrome C	Santa Cruz	Cat#sc-13156; RRID: AB_627385
Mouse monoclonal anti-β-tubulin	Developmental Studies Hybridoma Bank	Cat#E7; RRID: AB_2315513
Goat anti-mouse secondary antibody	LI-COR Biosciences	Cat#IRDye680; RRID: AB_621840
Goat anti-rabbit secondary antibody	LI-COR Biosciences	Cat#IRDye800CW; RRID: AB_621843
Anti-rabbit IgG	Cell Signaling Technology	Cat#7054; RRID: AB_2099235
Mouse monoclonal anti-5-hydroxymethylcytosine	Cell Signaling Technology	Cat#51660; RRID: AB_2799398
Rabbit monoclonal anti-5-methylcytosine	Cell Signaling Technology	Cat#28692; RRID: AB_2798962
Rabbit polyclonal anti-CD31	Thermo Fisher Scientific	Cat#PA5-24411; RRID: AB_2541911
Alexa Fluor 555-conjugated donkey anti-rabbit IgG	BioLegend	Cat#406412; RRID: AB_2563181
Mouse monoclonal anti-MYH I	Developmental Studies Hybridoma Bank	Cat#BA-F8; RRID: AB_10572253
Mouse monoclonal anti-MYH IIa	Developmental Studies Hybridoma Bank	Cat#SC-71; RRID: AB_2147165
Mouse monoclonal anti-MYH IIb	Developmental Studies Hybridoma Bank	Cat#BF-F3; RRID: AB_2266724
Alexa Fluor 488-conjugated goat anti-mouse IgG2b	Thermo Fisher Scientific	Cat#A-21141; RRID: AB_2535778
Alexa Fluor 555-conjugated goat anti-mouse IgG1	Thermo Fisher Scientific	Cat#A-21127; RRID: AB_2535769
Alexa Fluor 350-conjugated goat anti-mouse IgM	Thermo Fisher Scientific	Cat#A-31552; RRID: AB_2536169
Chemicals, Peptides, and Recombinant Proteins		
[Pyr1]apelin-13 peptide	AAPPTec	Lot#P181204-SY088340
Critical Commercial Assays		
BCA Protein Assay Kit II	BioVision	Cat#K813-2500; K813-5000
iScript™ cDNA Synthesis Kit	Bio-Rad	Cat#4106228
SsoAdvanced™ Universal SYBR Green Supermix	Bio-Rad	Cat#L001894A
Deposited Data		
RNA-seq data (fetal muscle WTTS-seq)	NCBI - SRA repository	SRA accession number: PRJNA674423
Experimental Models: Organisms/Strains		
C57BL/6J	Jackson Laboratory	Yang et al., 2016
$Apj^{Flox/flox}$	Dr. Kristy Red-Horse	Sharma et al., 2017
$β-actin^{Cre}$	Jackson Laboratory	Cat#019099

REAGENT or RESOURCE	SOURCE	IDENTIFIER
Software and Algorithms		
Oxymax for Windows v4.93	Columbus Instruments	Son et al., 2020
Odyssey Infrared Imaging System	LI-COR Biosciences	Son et al., 2019b
Image Studio Software v5.2.5	LI-COR Biosciences	Son et al., 2019b
EVOS® XL Core Imaging System	Thermo Fisher Scientific	Son et al., 2019b
ImageJ	National Institutes of Health	Son et al., 2020
Prism 7	GraphPad Software	N/A
SAS	SAS Institute Inc.	N/A
SPSS 21	IBM Corp.	N/A
Other		
Oxymax Fast 4 lane modular treadmill system	Columbus Instruments	Son et al., 2020
Grip strength meter	Columbus Instruments	Son et al., 2019b
Mouse diet, control diet, 10% energy from fat	Research Diets	D12450J
Mouse diet, high fat diet, 60% energy from fat	Research Diets	D12492